Eur Biophys J (2001) 30: 393–403
DOI 10.1007/s002490100153

ARTICLE

C.G. Scherk · A. Ostermann · K. Achterhold
O. Iakovleva · C. Nazikkol · B. Krebs · E.W. Knapp
W. Meyer-Klaucke · F.G. Parak

The X-ray absorption spectroscopy Debye-Waller factors of an iron compound and of met-myoglobin as a function of temperature

Received: 19 May 2000 / Revised version: 8 February 2001 / Accepted: 8 February 2001 / Published online: 10 August 2001

Abstract Protein dynamics can be characterized by the mean square displacements of the individual atoms of a molecule. This concept is extended to X-ray absorption spectroscopy (XAS) of proteins where the physical information in the Debye-Waller factor is in general neglected. In a first step, a procedure for the investigation of the temperature dependence of XAS spectra has been developed for a small iron compound. Subsequently, experiments have been performed on met-myoglobin. It is shown that the mean square displacements of XAS are smaller than those obtained by Mössbauer spectroscopy and far smaller than crystallographic mean square displacements. This behavior is explained by the different sensitivity of the methods. XAS measures a relative mean square displacement between the absorbing and backscattering atoms only. A comparison with mean square displacements calculated from normal modes shows that static displacements contribute significantly. It becomes obvious that the atoms of the active center show a high correlation of their motions.

Key words X-ray absorption spectroscopy · Protein dynamics · Debye-Waller factors · Temperature dependence · Metalloproteins

C.G. Scherk · A. Ostermann · K. Achterhold · O. Iakovleva
F.G. Parak (✉)
Physik Department E17 der Technischen Universität München,
85747 Garching, Germany
E-mail: fritz.parak@ph.tum.de
Fax: +49-89-28912548

C. Nazikkol · B. Krebs
Universität Münster, Anorganisch-chemisches Institut,
Wilhelm-Klemm-Strasse 8, 48149 Münster, Germany

E.W. Knapp
Freie Universität Berlin, FB Chemie,
Institut für Kristallographie,
Takustrasse 6, 14195 Berlin, Germany

W. Meyer-Klaucke
EMBL Hamburg, Notkestrasse 85,
22603 Hamburg, Germany

Introduction

The determination of the three-dimensional structure is an optimal starting point for the study of proteins. Acquiring precise data on the coordinates of the atoms is an important step for gaining information on these systems. However, for a deeper understanding of the function it is essential to study the dynamics. In recent years a lot of facts on protein dynamics has been accumulated. Data obtained from different techniques can be included in the discussion of, for example, X-ray structure analysis (Frauenfelder et al. 1979; Parak et al. 1987), Mössbauer studies (Parak and Frauenfelder 1993; Parak et al. 1981), neutron scattering (Doster et al. 1989), optical spectra (Di Pace et al. 1992), or Rayleigh scattering of Mössbauer radiation (Krupyanskii et al. 1982). X-ray absorption spectroscopy (XAS) is a technique which is now accepted as an important tool to display structural properties of proteins (Lee and Pendry 1975). It is mainly used to investigate the structure of active metal centers which cannot be or have not yet been investigated by X-ray structure analysis. Often it is used to study the effects of structural changes within the protein due to changes in the oxidation state or in pH (see Scherk et al. 1996). The XAS data analysis contains a Debye-Waller factor-like term which so far has often been reduced to just a "fitting parameter" (Beni and Platzman 1976), but is nowadays realized to be a valuable source of information (Dimakis and Bunker 1998; Poiarkova and Rehr 1999). Up to now this physical parameter was studied only in the case of "simple" molecules with few degrees of freedom [see for example Böhmer and Rabe 1979; Diop and Grisenti 1995 (for crystals); Stern 1987; Zhang et al. 1991 (for biomolecules)]. In principle, this factor opens up the possibility to study thermal fluctuations and static disorder which are displayed usually by the mean square displacements, $< x^2 >$, of the atoms.

Mean square displacements have been investigated for a long time. For small inorganic or organic

molecules the dynamics is mainly determined by the ionic or covalent binding of the atoms. Biomolecules, however, show a more complex behavior. The dynamics of myoglobin has been observed by Mössbauer spectroscopy (Parak and Formanek 1971; Parak et al. 1982). In deoxy-myoglobin above 180 K a dramatic increase of the mean square displacements, $<x^2>^{\gamma}$, of the heme iron was found. Mössbauer spectroscopy labels the protein dynamics on the position of the iron. All motional modes which couple to the Fe contribute to the $<x^2>^{\gamma}$ values. X-ray structure analysis yields information on all atoms if a refinement of individual mean square displacements, $<x_j^2>^{X}$, is performed for each non-hydrogen atom j (Artymiuk et al. 1979; Frauenfelder et al. 1979; Parak et al. 1987). The measurements are done on crystals containing typically 10^{15} molecules. Dynamic as well as static structural differences to the average structure contribute to $<x^2>^{X}$. In order to separate the static and dynamic parts of the $<x^2>^{X}$ values, the temperature can be lowered to freeze out the dynamics and obtain a value for the static contribution. Temperature-dependent studies on met-myoglobin crystals have been performed over a wide temperature range (between 80 K and 300 K) and showed a linear decrease with temperature (Parak et al. 1987).

In this paper the XAS Debye-Waller factor is treated as a physical quantity and not as a purely fitting parameter. XAS spectra of an iron compound with a molecular weight of 574.8 Da were measured at 20, 40, 70, 100, 150, 200, and 250 K. In addition, Mössbauer measurements of the same substance have been performed in the temperature range from 8 K to 280 K and the X-ray structure was solved at 150 K. These experiments were used to obtain a principle understanding. As a second step, experiments were performed on a met-myoglobin sample. The XAS spectra of met-myoglobin were taken at 40, 115, 185, and 260 K. A comparison of the results obtained by different techniques shows that the XAS Debye-Waller factors yield important complementary results. It should be stressed from the very beginning that XAS Debye-Waller factors measure only mean square displacements of the neighbors of the iron with respect to the iron.

Materials and methods

For XAS experiments on Fe, the iron compound [Fe(bbimae)acac]ClO_4 [$C_{23}H_{25}ClFeN_5O_7$] was synthesized (Nazikkol 1996). It has a molecular weight of 574.8 g/mol and, apart from the ClO_4 and Fe, it consists of 31 non-hydrogen atoms. The Fe^{3+} in the molecule center is six-fold coordinated by three oxygen and three nitrogen atoms (see Fig. 1). The material is produced in a microcrystalline, dry state. Mössbauer spectra were measured in a standard sample holder in an Oxford cryostat from 8 K to 280 K. The $<x^2>^{\gamma}$ values were obtained from the absorption area using the thin absorber approximation (Parak et al. 1982). For the X-ray structure determination a crystal was grown and measured at 150 K. The refinement was accomplished with SHELXL-93 (Sheldrick 1993).

The XAS was performed on the beamline D2 of the EMBL outstation at the DORIS storage ring, Hamburg. The sample was diluted with boron nitride (BN) in a ratio 1:5 to provide an absorption change $\Delta\mu x$ at the edge jump which is not too pronounced ($\Delta\mu x$ smaller than 1). A Si(111) double crystal monochromator was used to scan the synchrotron X-ray energies, allowing an energy resolution better than 1 eV. During the measurement the (111) reflection was detuned to reject higher harmonics. A mirror was used after the monochromator. The sample was cooled in a cryostat to the temperatures 20, 40, 70, 100, 150, 200, and 250 K. The K-edge spectra of the iron were recorded in absorption mode in a region up to 1400 eV above the absorption edge at 7112 eV (see Fig. 2). Individual scans were summed to improve statistics to allow an interpretation of the XAS spectra up to high energies. A large energy range is necessary since the widths and amplitudes in real space are determined by the effective k space – which represents the measured energy range – in which XAS occurs with significant amplitudes (Böhmer and Rabe 1979). The energy calibration was performed using the known reflections of a silicon crystal (Pettifer and Hermes 1985). The XAS data were analyzed by standard procedures used at the EMBL outstation, Hamburg (Nolting and Hermes 1992). The atomic absorption background was subtracted using a five-point cubic spline fit (see Fig. 3).

In the $k^3\chi(k)$ plot, as well as in the Fourier analysis, a decrease in intensities at higher temperatures can clearly be observed. The refinement of the XAS spectra was performed with the program package EXCURV92 (Binsted et al. 1991, 1992; Gurman 1988;

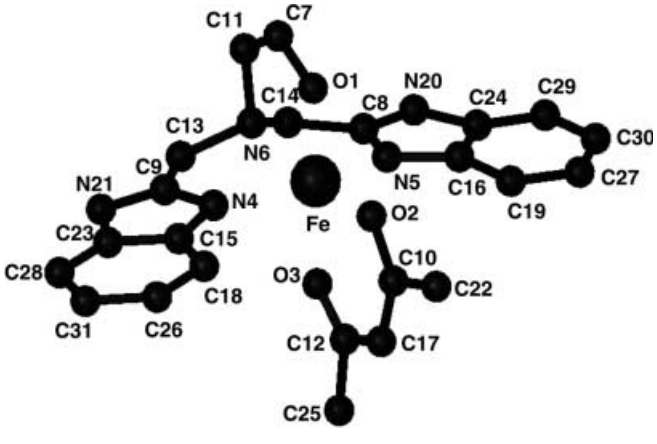

Fig. 1 X-ray structure of [Fe(bbimae)acac]ClO_4 (Nazikkol 1996). The atom numbers indicated here are referred to in the text

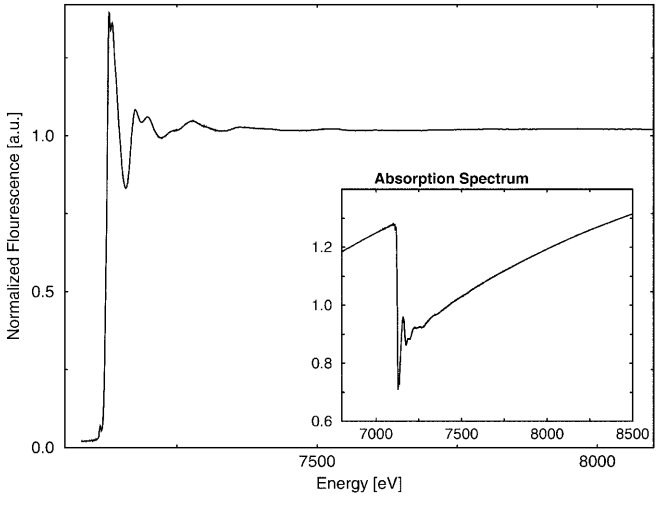

Fig. 2 Normalized absorption spectrum of [Fe(bbimae)acac]ClO_4 at 20 K. *Inset*: original absorption spectrum

Gurman et al. 1984, 1986; Joyner et al. 1987). In this process, all 31 atoms of the model compound were included in the calculation of the XAS spectra and arranged in scattering units. Multiple scattering up to three scattering processes was included. No Fourier filtering was used which could give rise to truncations and loss of information. The spectra were analyzed in k space (Lytle et al. 1989). The coordinates of the individual atoms were extracted from the X-ray structure analysis and kept constant during the analysis of the spectra. No refinement of the coordinates of the atoms was necessary to interpret the XAS spectra. Only the $<x^2>^{XAS}$ (in the EXCURV92 program referred to as A-values: $A = 2 < x^2 >^{XAS}$) of the atoms were determined in a least squares fit using a Marquardt fitting routine where the theoretical curve was iteratively adjusted to the experimental data (as well as the exact energy of the Fermi energy level E_F). The $<x^2>^{XAS}$ is included in the fitting routine in the exponential term $\exp[-2k^2 <x^2>^{XAS}]$. This term represents the effect of thermal motion of the atom (Beni and Platzman 1976) or structural disorder. To reduce the number of parameters and to avoid over-interpretation, the $<x^2>^{XAS}$ of atoms at similar geometric positions were combined and only varied together ($A1$, $A2 = A3$, $A4 = A5$, $A6$, $A7$, $A8 = A9$, $A10 = A12$, $A11$, $A13 = A14$, $A15 = A16$, $A17$, $A18 = A19$, $A20 = A21$, $A22 = A25$, $A23 = A24$, $A26 = A27$ and $A28 = A29 = A30 = A31$; the number after A refers to the atom number in Fig. 1). Together with the parameter E_F, this yields 18 fitted parameters. Mainly the atoms which are directly coordinating the iron center were adjusted individually (atoms 1–6). The so-called AFAC value, which accounts for amplitude losses due to shake up and off processes, was fixed to 0.85. In these processes, energy is deposited into excitation of electrons other than the absorbing one so that this absorption no longer contributes to the XAS amplitude. This value was obtained after extensive testing and was chosen to avoid negative A-values. Theoretical calculations propose a value of 0.69 (Teo 1986), which yields A-values at negative and therefore unphysical values.

Small crystals of met-myoglobin were grown according to the method of Kendrew and Parrish (1956). The sample was frozen in liquid nitrogen and equilibrated at the temperatures 40, 115, 185, and 260 K during the XAS measurements. The XAS spectra were taken again at the beamline D2 of the EMBL outstation at the DORIS storage ring, Hamburg. The same experimental setup was used as described above. The spectra were taken from 6900 eV to 8100 eV in the fluorescence mode using a 13 NaI scintillation counter array. Individual scans were added until the total number of fluorescence counts above the absorption edge accumulated to about 800,000 for each temperature spectrum (except 260 K). A modified strategy was used in measuring the spectra. To determine Debye-Waller factors, a good resolution at high energies is desirable. Therefore, the energy difference between two neighboring data points was kept constant. This results in an increased density of data points in the high k range after the transformation of the energy to k-space and yields, therefore, better statistics. After background subtraction the data points were redistributed to be equidistant on the k-scale. The measurement time was not increased dramatically by this approach, as it would have been if simply more scans had been taken.

Figures 4 and 5 show the original XAS spectra as well as the background subtracted spectra. The atomic absorption background was subtracted using a four-point cubic spline fit. The temperature effect can be seen especially in the Fourier transform of the XAS spectra (compare Fig. 5b). The first maximum clearly decreases.

The data were refined using the program EXCURV92 (Binsted et al. 1991, 1992; Gurman 1988; Gurman et al. 1984, 1986; Joyner et al. 1987). All atoms of the active center known from the X-ray structure (compare Fig. 6) are included, e.g. the porphyrin heme (24 atoms), the imidazole of a histidine (5 atoms), and a water molecule modeled by an oxygen atom ("XAS 30"). The AFAC value was set to the value used in the previous experiment. The strategy was again to use the coordinates of the X-ray structure analysis and to perform a refinement of the Debye-Waller factors only. In contrast to the small iron compound, it proved to be impossible to use the X-ray coordinates of the X-ray structures directly. The XAS spectra could not be reproduced correctly with these coordinates (see Fig. 7a and b). The radial positions are either insufficient to suit the XAS

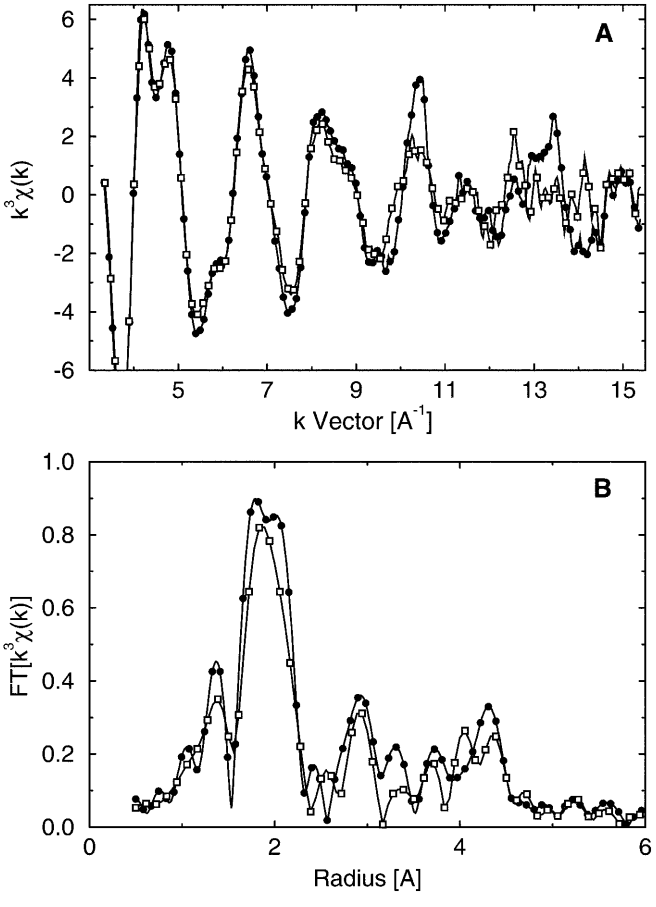

Fig. 3A, B Comparison of the XAS spectra of the iron compound at different temperatures: $T = 20$ K (*full circles*), $T = 250$ K (*open squares*). **A** k^3-weighted spectra; each third data point is given. **B** Fourier transformed spectra with equal window parameters

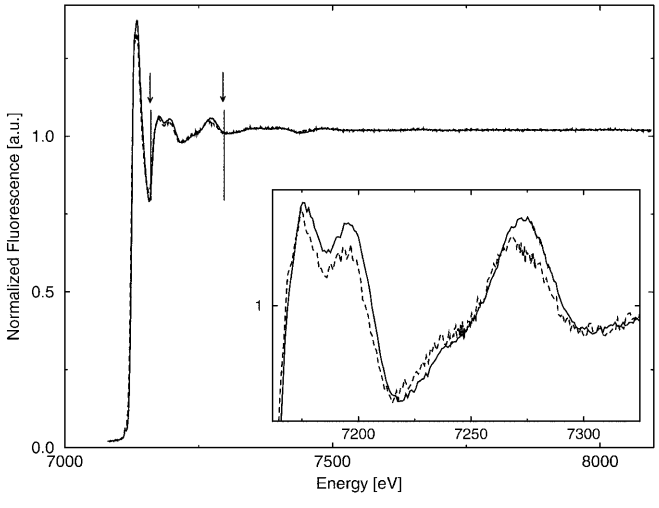

Fig. 4 Normalized fluorescence spectrum of met-myoglobin microcrystals at $T = 40$ K (*solid line*) and $T = 260$ K (*dashed line*). *Inset*: magnification of the first two oscillations of the XAS fine structure

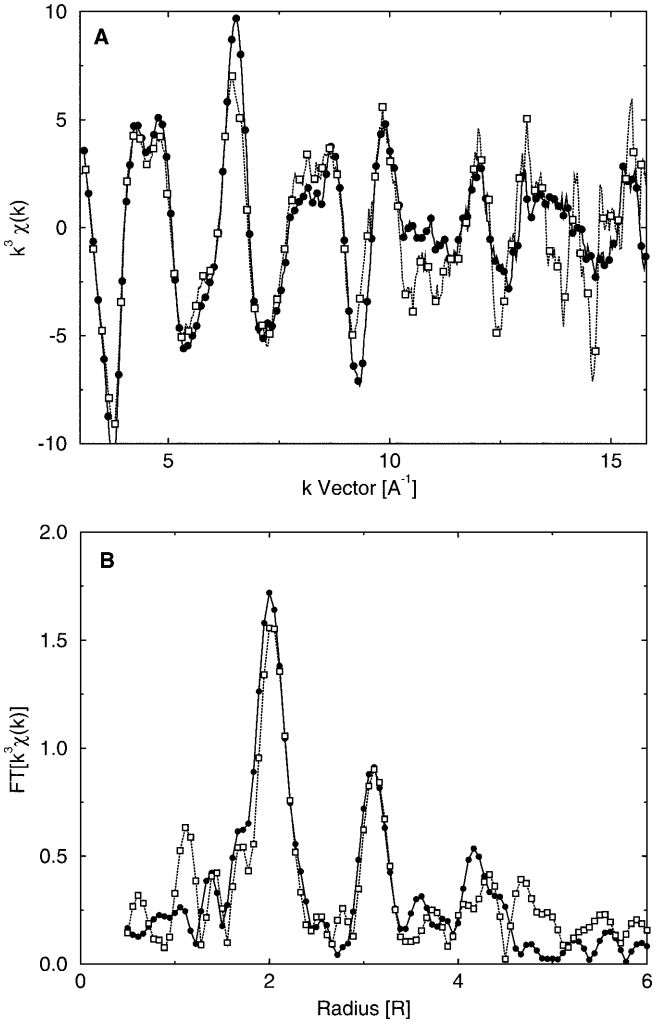

Fig. 5A, B Comparison of XAS spectra of met-myoglobin at the temperatures 40 K (*filled circles*) and 260 K (*open squares*). **A** k^3-weighted spectra; each third data point is given. **B** Fourier transformed spectra (exactly the same window parameters for both temperatures)

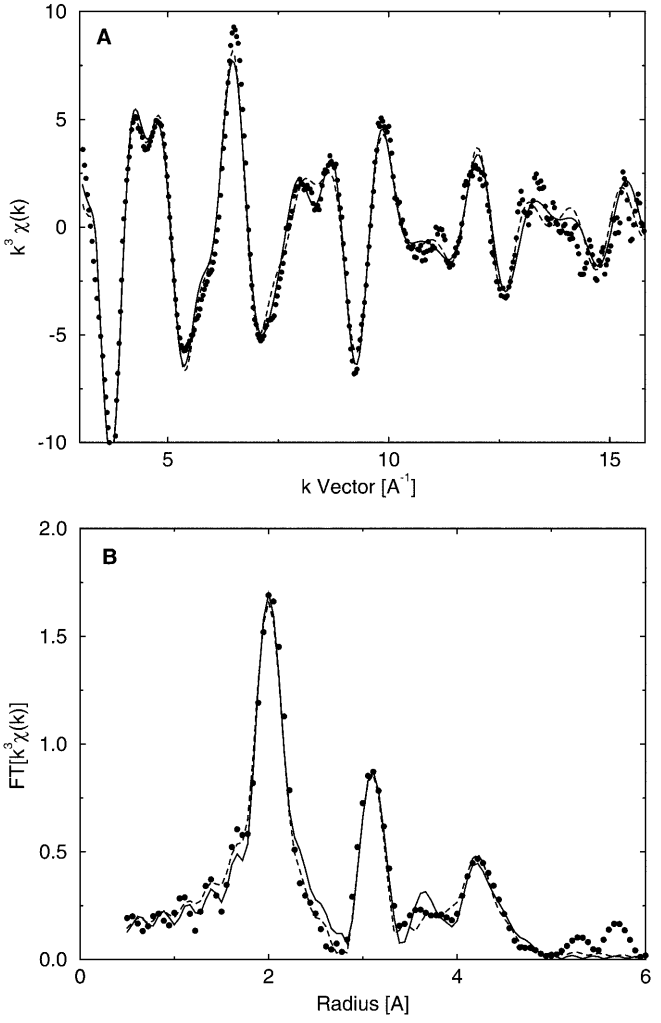

Fig. 7A, B XAS spectra at 115 K. *Dashed line*: a reduced pyrrole ring geometry is fitted ("XAS 12"); *solid line*: all atoms which are extracted from the X-ray structure are fitted ("XAS 30"). **A** k^3-weighted spectra. **B** Fourier transformed spectra

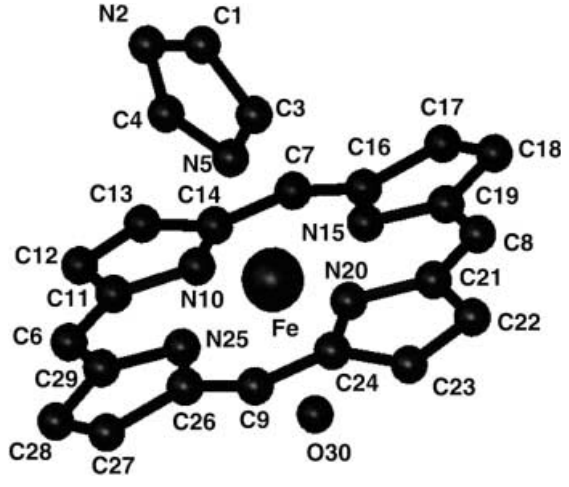

Fig. 6 The active center of met-myoglobin as obtained from X-ray crystallography. The atom numbers indicated here are referred to in the text

analysis or systematic errors have a pronounced effect which did not take place during the measurement of the iron compound (see Table 2). The main problem might be that the phase functions are calculated ab initio using Hedin-Lundquist potentials (Lee and Beni 1977). They might be not suitable enough in this case and might not reflect the protein phases correctly. In order to succeed in the following analysis, the *A*-values were fixed first and the radial distances of the imidazole, the four pyrrole rings contained in the heme, and the oxygen were constrained refined as well as a tilting angle of each group (Binsted et al. 1992). This angle was practically not changed compared to the original X-ray structural data. After the geometry at all four temperatures provided a satisfying fit of the spectra, the coordinates were fixed and only the *A*-values were varied. The latter are again combined in eight groups, reflecting similar positions in the complex (compare atom numbers given in Fig. 6; for the histidine $A1 = A2$, $A3 = A4$, $A5$ and the heme $A6 = A7 = A8 = A9$, $\boldsymbol{A10 = A15 = A20 = A25}$, $= A11 = A14 = A16 =$ $A19 = A24 = A26 = A29$, $A = 12 = A13 = A17 = A18 =$ $A22 = A22 = A27 = A28$, $\boldsymbol{A30}$). Parameters for the first coordination shell are printed bold. The combination of *A*-values into groups prevents specific factors to account only for noise in the spectra, while other factors are damped out.

In a second approach, a pyrrole ring with one methine group was extracted from the X-ray structure and weighted with a factor

of 4 ("XAS 12"). The imidazole ring and the water were not altered. This structure is constrained refined and subsequently, after fixing the structure, the *A*-values are varied in eight groups ($A1 = A2$, $A3 = A4$, ***A5***, $4\times A6$, ***4×A10***, $4\times A11 = A14$, $4\times A12 = A13$, ***A30***). Figure 7 shows the final fitting results for the 115 K spectra for both approaches. Both techniques yield approximately the same quality in the fits.

Results

In this paper the mean square displacements measured by different methods are compared on a small iron compound and on met-myoglobin. To avoid confusion we talk only about mean square displacements $< x^2 >$. The experimental method is indicated as upper index where X characterizes X-ray structure determination, XAS the X-ray absorption spectroscopy, γ the Mössbauer spectroscopy, and NM the normal mode analysis. We use:

$$< x^2 >^{\mathrm{X}} = B/(8\pi^2); \quad < x^2 >^{\mathrm{XAS}} = A/2 = \sigma^2 \qquad (1)$$

where B is the crystallographic B-factor, and A and σ are the commonly used parameters of XAS (Beni and Platzman 1976; Binsted et al. 1991, 1992; Gurman 1988; Gurman et al. 1984, 1986; Joyner et al. 1987). In optical absorption experiments a considerable fraction of the variance of the broadening of the Gaussian lineshape σ^2_{Opt} of the Soret band arises from line broadening due to coupling of the electronic transition with low-frequency vibrational modes (Cupane et al. 1995). The $< x^2 >^{\mathrm{opt}}$ can be deduced from σ^2_{Opt} according to Melchers et al. (1996).

Mean square displacements in the iron compound

The coordinates given by the X-ray structure are very accurate, with uncertainties of less than 1%, e.g. smaller than 0.01 Å (Nazikkol 1996; see Table 1). With these coordinates the XAS spectra were fitted without any adjustment. It is a strong justification of the XAS technique that these spectra can be understood with the exact coordinates obtained from the X-ray structure. The EXCURV92 program, for example, uses ab initio phase and potential calculations which obviously satisfy the required accuracy. Only a few parameters have been varied to simulate the spectra using the constraints theory given above (an energy offset and the *A*-values, see Materials and methods section). The main problem of the refinement lies in the correlation of the parameters. Mean square displacements of atoms sited at the same distance from the absorbing atom tend to compensate each other's contributions. This means that if one of these atoms is forced to a very small $< x^2 >^{\mathrm{XAS}}$, the contribution of another one is almost canceled (huge $< x^2 >^{\mathrm{XAS}}$). This makes necessary a correlation to $< x^2 >^{\mathrm{XAS}}$ of individual atoms which have similar structural positions. However, this procedure cancels individual contributions of single atoms as such. Particularly for atoms which are at a distance more than 3 Å away from the iron atom, the experimental statistics are too poor to separate individual contributions of atoms even for the model compound. The competition between noise and the real backscattering contribution is not negligible. In addition, multiple-scattering contributions from the first and second shells dominate in the Fourier transform at about 4 Å (compare Fig. 3). Therefore, only the atoms in the first coordination shell will be discussed in detail. The best fit for a XAS spectrum is obtained at temperatures around 150 K. If one goes to lower temperatures, as well as to higher ones, the *R*-value of the refinement increases. It is not surprising that the coordinates of the atoms fit the 150 K spectrum in the best way since the structure was determined at this temperature. It also means that the resulting mean square displacements at higher and lower temperatures

Table 1 Results for the iron compound. For the first shell atoms the radial distance, R_j, from the absorbing iron atom was used as obtained from the crystal structure (second column). For the atoms the $< x^2 >$ values at different temperatures are given. Columns 3–9 refer to XAS measurements and column 10 to the X-ray structure determination. $< 1\text{–}6 >$ gives $< x^2 >$ values averaged over the atoms 1 to 6. $< x^2 >$ values obtained by Mössbauer spectroscopy are added in the line below. The last two lines give the *R*-factor of the XAS fits and the fitted Fermi energies, E_{F}, for the XAS experiments at different temperatures

Atom	R_j (Å)	$< x^2 >$ (Å^2)							
		XAS							X-ray
		20 K	40 K	70 K	100 K	150 K	200 K	250 K	150 K
Fe	0.000	–	–	–	–	–	–	–	0.0213
O_1	1.901	0.0007	0.0008	0.0009	0.0008	0.0020	0.0024	0.0030	0.0233
O_2	1.942	0.0008	0.0010	0.0013	0.0017	0.0015	0.0020	0.0014	0.0322
O_3	2.049	0.0008	0.0010	0.0013	0.0017	0.0015	0.0020	0.0014	0.0297
N_4	2.078	0.0018	0.0019	0.0019	0.0019	0.0033	0.0040	0.0064	0.0211
N_5	2.088	0.0018	0.0019	0.0019	0.0019	0.0033	0.0040	0.0064	0.0211
N_6	2.303	0.0015	0.0013	0.0018	0.0021	0.0033	0.0054	0.0100	0.0201
$< 1\text{–}6 >$	–	0.0012	0.0013	0.0015	0.0017	0.0025	0.0033	0.0048	0.0241
Mössbauer $< x^2 >^{\gamma}$		0.0050	0.0063	0.0090	0.0115	0.0160	0.0211	0.0265	–
R_{fact}		44.16	38.58	40.21	38.42	38.70	45.33	46.18	–
E_{F} (eV)		–6.746	–6.766	–6.788	–6.788	–6.582	–6.595	–6.337	–

contain static contributions which reflect differences of the structure at the measured temperature from the structure at 150 K. In any case, these contributions are not very large; for example, if one obtains a shift of $\Delta x = 0.01$ Å it gives a contribution of 0.0001 Å^2 to $< x^2 >$.

The results of the analysis of the model compound are shown in Fig. 8 and given in Table 1. The $< x^2 >^X$ for the six nearest atoms to the iron at 150 K are in the range between 0.020 and 0.032 Å^2 with an error smaller than 0.001 Å^2. In general, one can observe that the atoms with the smallest $< x^2 >^X$ are sited in the center of the molecule, which means around the iron atom. The further an atom is located away from the iron, the bigger is the $< x^2 >^X$ in general. The $< x^2 >^\gamma$ value at 150 K is only about 20% smaller than the $< x^2 >^X$ for the iron atom. Compared to these results, the $< x^2 >^{XAS}$ values are almost a factor of 5 smaller than those determined by Mössbauer spectroscopy (compare Table 1). They show an increase with temperature from 0.001 Å^2 at 20 K to 0.005 Å^2 at 250 K for the averaged first coordination shell. The errors of the fit are estimated to be ± 0.001 Å^2.

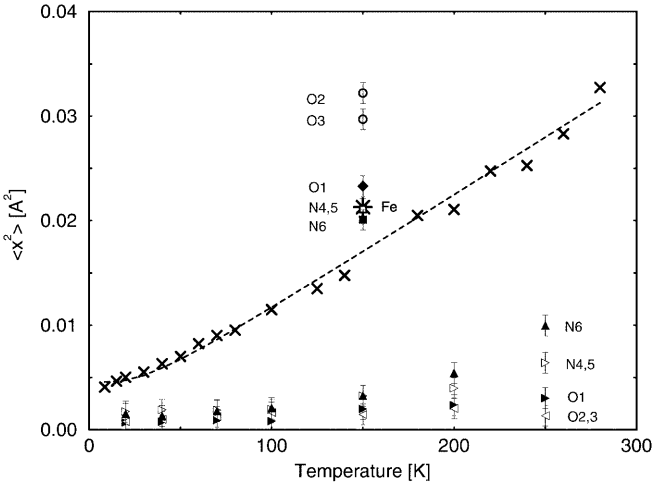

Fig. 8 Model compound: mean square displacements for the different atoms measured by different techniques as a function of temperature. X-ray structure determination: Fe (*star*), O_1 (*filled diamond*), O_2 and O_3 (*open circles*), N_4 and N_5 (*open square*), N_6 (*filled square*). Mössbauer mean square displacement of Fe (*crosses*). *Dashed line*: least squares fit by a hyperbolic cotangent function. XAS mean square displacements for first shell atoms: O_1 and N_6 (*filled triangles*), O_2/O_3 and N_4/N_5 (*open triangles*)

Mean square displacements in met-myoglobin

Owing to the size of a protein, the derived values have greater uncertainties than those of a simple complex. Again, only the first coordination shell is discussed (from the histidine the atom N_5, the four pyrrole ring nitrogens N_{10}, N_{15}, N_{20}, N_{25}, and the water O_{30}; see Table 3). The XAS analysis shows an increase in the average distance of the pyrrole ring nitrogens with higher temperatures, whereas the distances of the water molecule and the histidine nitrogen stay approximately at the same distance (see Table 2). This behavior is revealed in both evaluation approaches applied, e.g. the fit with all individual atoms as well as with one pyrrole ring weighted with a factor of 4. In contrast to the X-ray structure investigations, all pyrrole nitrogens seem to be located at similar distances from the iron atom. This fact can be deduced empirically from examination of the first Fourier maximum, which is apparently not split (compare Fig. 5b). In the X-ray structure at a certain temperature the distances of the pyrrole ring nitrogens from the iron atom can differ by up to 0.18 Å. Nevertheless, in addition to this observation, a systematic difference can be detected between XAS and the X-ray structures: the iron-pyrrole ring distance is on average always about 0.03 Å larger in the XAS investigation; the effect can be seen in Fig. 7b in the position of the first Fourier maximum.

Table 2 Structural parameters of the first shell atoms used in refining met-myoglobin; X-ray denotes the X-ray structures (Parak et al. 1987); in "XAS 30" the refinement of all 30 atoms of the active center are included; in "XAS 12" are fitted only 12 atoms, with four times the contribution of one pyrrole ring (here R_{10}); the angles TH_2, TH_{13}, TH_{18}, TH_{23}, and TH_{28} display the orientation of the ligands, R_{fact} is the fitting index as given in Binsted et al. (1992); E_F is the offset of the absorption energy

	40 K			115 K			185 K			260 K		
	X-ray	XAS 30	XAS 12	X-ray	XAS 30	XAS 12	X-ray	XAS 30	XAS 12	X-ray	XAS 30	XAS 12
R_{fact}	–	29.43	28.59	–	29.26	28.44	–	31.94	30.75	–	45.30	45.65
E_F (eV)	–	–6.65	–6.82	–	–7.02	–6.82	–	–6.85	–7.23	–	–5.72	–6.50
R_5 (Å)	2.205	2.125	2.115	2.267	2.135	2.120	2.172	2.139	2.130	2.224	2.120	2.120
R_{10} (Å)	2.004	2.013	2.017	1.969	2.022	2.023	2.003	2.022	2.031	1.970	2.037	2.044
R_{15} (Å)	1.915	2.035	–	1.976	2.026	–	1.997	2.021	–	2.009	2.053	–
R_{20} (Å)	2.098	2.014	–	1.986	2.031	–	2.000	2.030	–	1.988	2.053	–
R_{25} (Å)	1.920	2.024	–	1.946	2.031	–	2.001	2.044	–	1.998	2.044	–
R_{30} (Å)	2.065	2.107	2.098	2.126	2.109	2.109	2.236	2.102	2.109	2.195	2.101	2.101
TH_2 (°)	94.4	98.6	–	94.5	97.1	–	94.6	98.5	–	96.3	98.2	
TH_{13} (°)	32.8	33.5	–	31.8	33.6	–	34.6	32.9	–	34.8	36.3	
TH_{18} (°)	58.8	58.8	–	56.9	58.8	–	59.1	55.8	–	59.5	58.5	
TH_{23} (°)	144.3	143.1	–	144.3	142.5	–	145.8	143.1	–	143.4	142.9	
TH_{28} (°)	119.2	119.3	–	118.9	120.1	–	119.6	119.0	–	119.5	119.4	

The $<x^2>^{XAS}$ values averaged over the first shell atoms change from 0.002 Å^2 at 40 K to 0.007 Å^2 at 260 K (see Table 3). Similar results are obtained by both refinement methods applied, e.g. whether all atoms are included explicitly or a reduced geometry is used. In the latter case a static disorder contribution to $<x^2>^{XAS}$, which results from the averaging over the individual pyrrole ring distances, should be increased. Since all different pyrrole rings are located at similar distances from the iron center (see Table 2), this contribution seems to be negligible. The error bars of such an investigation stretch over a broad range. For the atoms of the first coordination shell they can be estimated from the fit as ± 0.001 Å^2 for the pyrrole nitrogens and ± 0.005 Å^2 for the histidine nitrogen or the water molecule. This means that even for the nearest atoms the errors are in the range of the values themselves. For atoms which are located at greater distances from the iron, this statement is even more valid, particularly if the contribution of these atoms to the XAS amplitude is close to the noise level of the measurement.

For comparison, Mössbauer experiments have been performed on met-myoglobin. The obtained mean square displacements show a fairly linear temperature dependence below about 200 K and a clear increase above this temperature.

Recently, data from temperature-dependent X-ray structure determinations of met-myoglobin have been analyzed by a normal mode refinement (Parak et al. 1999). This method allows the separation of internal modes of motions from translation, libration, and screwing (Kidera and Go 1992). Figure 9 gives the mean square displacement of the iron atom, caused only by internal motions.

Discussion

In order to obtain physical information on the dynamical properties of molecules, several experimental methods have to be applied. In this paper, different techniques are compared which are available to study the mean square displacement, $<x^2>$. We assume that the experimentally obtained mean square displacements are isotropic and, thus, the validity of the relation:

$$<r^2>=<x^2>+<y^2>+<z^2>=3<x^2> \qquad (2)$$

In both the iron compound and in met-myoglobin the $<x^2>^{XAS}$ values are well below the $<x^2>^{\gamma}$ and $<x^2>^{X}$ values, which comes from the following fact: $<x^2>^{XAS}$ measures exclusively the relative mean square displacement between the absorbing atom and a backscattering atom j along the connecting vector $\boldsymbol{R}_j$ (Beni and Platzman 1976; Sevillano at al. 1979). Only relative motions or displacements between the absorbing and the backscattering atoms have to be taken into account. It has to be emphasized that TLS motions (translation, libration, screwing), which move the molecule like a rigid body, do not contribute to $<x^2>^{XAS}$. TLS motions do not change the distance of the iron from the neighboring atoms. The approximation used in the following is valid for vibrations which are described by a harmonic Hamiltonian. In this case the necessary ensemble average can be calculated. If $\boldsymbol{u}_{Fe}$ represents the displacement of the absorbing iron atom, $\boldsymbol{u}_j$ the displacement of the backscattering atom j, the mean square relative displacement can be written as

$$<x^2>^{XAS}=<[(\boldsymbol{u}_{Fe}^{-\boldsymbol{u}_j})\boldsymbol{e}_R]^2>=<(\boldsymbol{u}_{Fe}\boldsymbol{e}_R)^2> +<(\boldsymbol{u}_j\boldsymbol{e}_R)^2>-2<(\boldsymbol{u}_{Fe}\boldsymbol{e}_R(\boldsymbol{u}_j\boldsymbol{e}_R)> \qquad (3)$$

with $\boldsymbol{e}_R=\boldsymbol{R}_j/|\boldsymbol{R}_j|$. This equation represents the mean square displacements of the absorbing iron and the backscattering atoms, which are projected on their connecting vector. Any common displacement from the average position, which is characterized by the third term, is subtracted. XAS measures the projection of the motional mode on the vector $\boldsymbol{e}_R$ which is a unit vector from the absorbing to backscattering atoms independent of the orientation of the molecule towards the incoming beam. Thus, the first term on the right-hand side of Eq. (3) becomes $<(\boldsymbol{u}_{Fe}\boldsymbol{e}_R)^2>=<|\boldsymbol{u}_{Fe}|^2\cos^2\alpha>$, where α is the angle between $\boldsymbol{e}_R$ and $\boldsymbol{u}_{Fe}$. Let us discuss some relevant cases. If one assumes an isotropic distribution of motional modes, e.g. there exist modes with the same amplitude $|\boldsymbol{u}_{Fe}|$ in all space directions, again a spherical

Table 3 Mean square displacements for met-myoglobin are given at different temperatures. In the first column the Mössbauer $<x^2>^{\gamma}$ values are displayed. Columns 3–6 show the XAS $<x^2>^{XAS}$ values of the first-shell atoms of met-myoglobin, where all 30 atoms of the active center are included ("XAS 30") in the refinement. The $<x^2>^{XAS}$ values of the atoms N_{10}, N_{15}, N_{20}, N_{25} are combined. "Ligands average" is the average over atoms 5, 10, 15, 20, 25, and 30 as shown in Fig. 9. Columns 7–10 give the results of the $<x^2>^{XAS}$ refinement, where only 12 independent atoms were included ("XAS 12") in the refinement

T (K)	$<x^2>^{\gamma}$ (Å^2)	$<x^2>^{XAS}$ (Å^2)							
	Fe	XAS 30				XAS 12			
		N_5	N_{10}, N_{15} N_{20}, N_{25}	O_{30}	Ligands average	N_5	N_{10}, N_{15} N_{20}, N_{25}	O_{30}	Ligands average
40	0.0026	0.0018	0.0019	0.0043	0.0026	0.0017	0.0023	0.0030	0.0023
115	0.0063	0.0033	0.0023	0.0044	0.0022	0.0024	0.0025	0.0032	0.0027
185	0.0121	0.0044	0.0025	0.0047	0.0029	0.0028	0.0027	0.0050	0.0035
260	0.0334	0.0062	0.0032	0.0125	0.0073	0.0062	0.0032	0.0125	0.0073

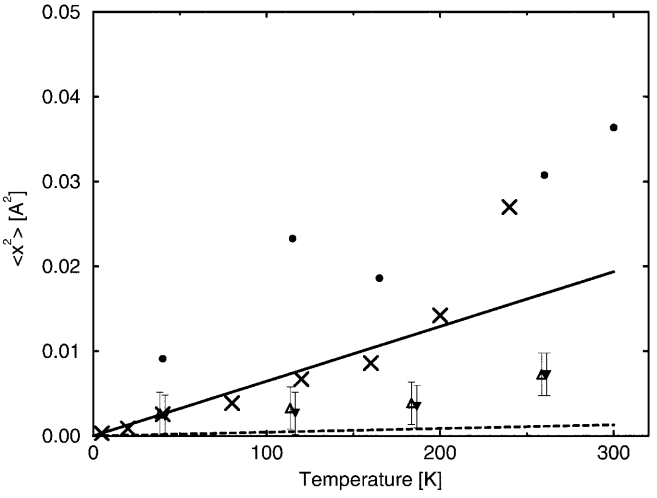

Fig. 9 Met-myoglobin: mean square displacements determined by different techniques as a function of temperature. XAS values for the nearest neighbors of iron: refinement XAS 30 (*open triangles*), refinement XAS 12 (*filled triangles*). Mössbauer mean square displacement of iron in met-myoglobin (*crosses*). Crystallographic mean square displacements $<x^2>^{X}$ of the iron for the internal motions (*full circles*). Normal mode analysis: iron in met-myoglobin (*solid line*), iron-histidine modes (*dashed line*)

average is performed and $<|\boldsymbol{u}_{Fe}|^2\cos^2\alpha>=(1/3)<|\boldsymbol{u}_{Fe}|^2>=<x^2>$. In the case of strong anisotropic motion, this assumption no longer holds. If there is only one dominant motional direction, so that we can neglect all other motions, the result becomes $<(\boldsymbol{u}_{Fe}\boldsymbol{e}_R)^2>=<|\boldsymbol{u}_{Fe}|^2>\cos^2\alpha$. Thus $<(\boldsymbol{u}_{Fe}\boldsymbol{e}_R)^2>$ ranges between zero for a mode which is perpendicular to $\boldsymbol{e}_R$ and $3<x^2>^{\gamma}$ if the mode is parallel to $\boldsymbol{e}_R$. The same considerations have to be taken into account when discussing the last two terms in Eq. (3). Additionally, if $\boldsymbol{u}_{Fe}=\boldsymbol{u}_j$, the resulting $<x^2>^{XAS}$ becomes zero since the correlation term cancels the first two contributions. For a strong correlated motion against each other ($\boldsymbol{u}_{Fe}=-\boldsymbol{u}_j$), the maximum possible value is obtained ($6<x^2>^{\gamma}+6<x_j^2>$). The $<x^2>^{XAS}$ yields half of that value if $|\boldsymbol{u}_{Fe}|=|\boldsymbol{u}_j|$, $\alpha=0$, and if there is no correlation at all between the motion of the absorbing and the backscattering atoms. However, the last two cases seem to be unrealistic for two atoms which are bound in a large complex.

The $<x^2>^{XAS}$ also accounts for static disorder varying the distance of the iron to its neighbors. This is particularly the case when a number of atoms surrounding the iron are represented by one single shell. The deviation of the actual position of the atoms enters directly into $<x^2>^{XAS}$. For the myoglobin sample the porphyrin ring was simulated by one single pyrrole ring with weight factor 4. An assumed deviation of the single nitrogens to the fitted distance of 0.02 Å results in an addition to $<x^2>^{XAS}$ of 0.0004 Å^2, which is practically negligible. It is at least a factor of 5 less than the obtained values at 40 K. However, this is not necessarily always the case. Here, it is assumed that the pyrrole ring is highly symmetric.

The information from XAS on the mean square displacement needs to be compared to already available data. In Mössbauer spectroscopy the $<x^2>^{\gamma}$ measures all dynamical processes which occur on a time scale faster than 141 ns, the lifetime of the Mössbauer ^{57}Fe nucleus (Mössbauer 1987; Mössbauer and Sharp 1964). Mössbauer absorption spectroscopy is only sensitive to the motions of the iron atom in the direction of the incident beam. In a powder sample a spherical average over each motional mode is accomplished, which yields a factor of 1/3, e.g. the $<x^2>$ is measured rather than the $<r^2>$.

The mean square displacements, $<x^2>^{X}$, determined by X-ray crystallography are obtained from the intensities of the Bragg reflections. All atoms of the crystal contribute coherently. The scattering occurs instantaneously. Therefore, the $<x^2>^{X}$ values represent all displacements of an atom from its average position in the unit cell. Static contributions and dynamics on all time scales are not distinguished. The different sensitivities of the methods reflect themselves in the different $<x^2>$ values obtained from the experiments. TLS motions contribute and have to be separated by normal mode refinement (Parak et al. 1999).

We first discuss the small iron compound. At 150 K the $<x^2>^{X}$ value is only slightly larger than the $<x^2>^{\gamma}$ value of the iron (compare Fig. 8). Since the $<x^2>^{\gamma}$ value stems from dynamical contributions only, one can conclude that structural disorder plays no important role in this compound. All molecules in the crystal have a nearly identical structure. The mean square displacements obtained from Mössbauer spectroscopy can be fitted with a cotangent hyperbolic law according to:

$$<x^2>(T)=\frac{\hbar}{m_{Fe}\omega}\frac{1}{2}\coth(\hbar\omega/2k_BT)=<x_v^2> \qquad (4)$$

where m_{Fe} is the mass of iron, $\hbar$ and k_B are the Planck and Boltzmann constants, and ω is a characteristic frequency. This fit proves that only harmonic motions are involved. The comparison of X-ray and Mössbauer data shows that most of the mean square displacements stem from motions. The small $<x^2>^{XAS}$ values are reasonable since only relative motions or displacements with respect to the iron are involved. A comparison with the $<x^2>^{\gamma}$ values proves that the total motion of the iron with respect to the laboratory system is mainly caused by common displacements together with the next neighbors. Astonishingly, the absolute $<x^2>^{XAS}$ values are close to those of myoglobin. As we shall discuss below, this means that static displacements also contribute.

In the case of myoglobin, the situation is more complicated. Proteins can exist in different conformational substates (Austin et al. 1975). Therefore, in X-ray crystallography, $<x^2>^{X}$ can be decomposed into three contributions:

$$<x^2>^{X}=<x_v^2>+<x_{ct}^2>+<x_{TLS}^2> \qquad (5)$$

The $<x^2_v>$ part reflects internal motions within the molecule. The $<x^2_{ct}>$ term accounts for different conformational substates. In each substate the structure might differ a little from the average structure. A specific molecule may be frozen in a conformational substate or jump between substates; in both cases the mean square displacement is increased by $<x^2_{ct}>$. Finally, $<x^2_{TLS}>$ reflects the fact that a protein as a whole may be displaced with regard to its averaged position in the crystal. In small compounds like our iron compound, $<x^2_{TLS}>$ is neglected.

The difference in $<x^2>^{\gamma}$ and $<x^2>^{X}$ for the iron in myoglobin is much larger than in the small iron compound. This is due to the mentioned conformational substates. Note that, in Fig. 9, only the internal modes at the position of the iron are given. The contribution of TLS is already subtracted from the original $<x^2>^{X}$ values.

For deoxy-myoglobin it was shown (Melchers et al. 1996) that the $<x^2>^{\gamma}$ values of the iron can be explained by normal modes at temperatures below 180 K. This yields, in Eq. (4), $<x^2_v> = <x^2>^{\gamma} = <x^2>^{NM}$. Recently, the normal mode analysis was also performed on met-myoglobin (Parak et al. 1999). As shown in Fig. 9, the agreement with the low-temperature Mössbauer mean square displacements of met-myoglobin is astonishingly good. Above 200 K, protein-specific motions become activated and give rise to the protein-specific increase of $<x^2>^{\gamma}$. They can be understood as a diffusion in limited space; see Cohen et al. (1981), Parak et al. (1981), and Parak et al. (1982).

For the calculation of EXAFS Debye-Waller factors, various techniques are in use (Dimakis and Bunker 1998; Poiarkova and Rehr 1999). In the following we use the normal modes to analyze the $<x^2>^{XAS}$ values. Melchers et al. (1996) provides the normal mode k of the atom i with the energy $\hbar\omega_k$, mass m_i and the eigenvector $\boldsymbol{d}_i^k$. The mean square displacement $<x^2>^{NM}$ is then in the classical approximation:

$$<(x_i^k)^2>^{NM} = \frac{1}{3}(\boldsymbol{d}_i^k)^2 \frac{k_B T}{m_i \omega_k^2} \tag{6}$$

If one wants to calculate the relative $<x^2>^{NM}$ from this expression, the contributions of the individual modes have to be summed. In the case of a directed motion along a vector $\boldsymbol{e}_R$ (in XAS the unit vector from the absorbing Fe to the backscattering atom i) this sum becomes:

$$<x^2_{i,Fe}>^{NM}_{Rel} = \frac{1}{3}\sum_{k=7,\ldots}\left\langle\left(\boldsymbol{d}^k_{Fe}\sqrt{\frac{k_B T}{m_{Fe}\omega_k^2}} - \boldsymbol{d}^k_i\sqrt{\frac{k_B T}{m_i\omega_k^2}}\right)\boldsymbol{e}_R\right\rangle^2 \tag{7}$$

The phase relation in the motion between the absorbing and the scattering atoms is maintained. The normal mode analysis yields in total 6219 frequencies, which correspond to the normal motions of the protein. About five low-frequency modes account for over 30% of the $<x^2>^{NM}$ (7.11 cm^{-1}, 8.31 cm^{-1}, 9.26 cm^{-1}, 10.85 cm^{-1}, 12.19 cm^{-1}). The rest of the $<x^2>^{NM}$ is produced by the vast majority of the modes, with each of the modes contributing a very small part to the $<x^2>^{NM}$. This picture changes drastically if one observes the relative $<x^2>^{NM}_{Rel}$, taking into account only the relative motions between the iron and its ligands. Between the iron and the histidine there exists not even one remaining frequency which would contribute more than 2% to $<x^2>^{NM}_{Rel}$. Apparently, the iron and the histidine move essentially in phase. Between the iron and the porphyrin ring there exists only one normal mode at 10.85 cm^{-1}, which accounts for about 10% of the $<x^2>^{NM}_{Rel}$. This frequency represents the only motion between the iron and the porphyrin ring. The rest of the normal modes form a quasi-isotropic background, which produces the major part of $<x^2>^{NM}_{Rel}$.

We first compare $<x^2>^{NM}$ and $<x^2>^{NM}_{Rel}$, which both are a result of the normal mode analysis since only normal mode displacements of the neighbors of the iron with respect to the iron ($<x^2>^{NM}_{Rel}$) can be compared with $<x^2>^{XAS}$. The majority of the motions of the active center are correlated motions where the iron and the neighbor atoms move practically in phase. There are hints from the XAS experiments that the motions normal to the heme plane between the iron and the histidine are more pronounced than inside the heme plane, since the $<x^2>^{XAS}$ of N_5 is bigger than those of N_{10}, N_{15}, N_{20}, or N_{25} (see Table 3). The iron seems to be strongly fixed within the borders defined by the porphyrin ring. This is in good agreement with results from Mössbauer spectroscopy (Afanas'ev et al. 1987; Nazikkol 1996). It is, however, rather difficult to make more detailed conclusions. The large errors of the individual $<x^2>^{XAS}$ values limit the interpretation. While the normal mode analysis accounts quite well for the total motion of the iron, determined by Mössbauer spectroscopy, the relative mean square displacements calculated from the normal mode analysis are much smaller than the experimentally obtained $<x^2>^{XAS}$ values (see Fig. 9). This shows that static distortions contribute significantly. This is again a hint that conformational substates are important.

Protein-specific motions reveal themselves by the strong increase of $<x^2>^{\gamma}$ above 180 K. The $<x^2>^{XAS}$ values do not show such behavior. According to Parak et al. (1982), quasi-diffusive motions of segments of the protein molecule are activated above 180 K. Such motions are highly correlated and do not contribute to $<x^2>^{XAS}$.

The XAS values can also be compared to optical ones. In the case of myoglobin, optical spectroscopy observes only the relative motion of the iron atom with respect to the heme plane (Melchers et al. 1996). The optical mean square displacements range from 0.001 $Å^2$ at 40 K to 0.003 $Å^2$ at 250 K in the case of deoxy-myoglobin. This is far below the $<x^2>^{XAS}$ values. Here

we see again that the $<x^2>^{XAS}$ is strongly influenced by conformational substates, yielding the term $<x^2_{ct}>$ in Eq. (5).

Conclusions

For a comparison of $<x^2>^{XAS}$ values with $<x^2>$ values obtained by other methods, one has to have in mind that only relative displacements between the iron and it nearest neighbors contribute to $<x^2>^{XAS}$. Compared with $<x^2>^{X}$ values the $<x^2>^{XAS}$ values are significantly smaller in both compounds. This reflects the fact that X-ray Debye-Waller factors are sensitive to all displacements, including displacements which do not change the relative distance of the iron from its neighbors. If all $<x^2>^{XAS}$ displacements came from dynamic effects, they should be smaller than $<x^2>^{\gamma}$ and equal to $<x^2>^{NM}_{Rel}$. However, in myoglobin they are significantly larger. This shows that static disorder strongly contributes as a consequence of conformational substates in proteins.

Acknowledgements This work was supported by the BMBF (project 05 649 WOA 4) and the Fonds der Chemie.

References

Afanas'ev AM, Tsymbal EYu, Cherepanov VM, Chuev NA, Yakimov SS, Parak F (1987) Effect of spin-lattice relaxation on the Mössbauer spectrum of metmyoglobin. Sov Phys JETP 65:1246–1251

Artymiuk PJ, Blake CCF, Grace DEP, Oatley SJ, Phillips DC, Sternberg MJE (1979) Crystallographic studies of dynamic properties of lysozyme. Nature 280:563–568

Austin A, Beeson K, Eisenstein L, Frauenfelder H, Gunsalus I, Marshall V (1975) Dynamics of ligand binding to myoglobin. Biochemistry 14:5355–5373

Beni G, Platzman PM (1976) Temperature and polarization dependence of extended x-ray absorption fine structure spectra. Phys Rev B 14:1514–1518

Binsted N, Campbell JW, Gurman SJ, Stephenson PC (1991) SERC Daresbury Laboratory, EXCURV92 program

Binsted N, Strange RW, Hasnain SS (1992) Constrained and restrained refinement in EXAFS data analysis with curved wave theory. Biochemistry 31:12117–12125

Böhmer W, Rabe P (1979) Temperature dependence of the mean square relative displacements of nearest-neighbour atoms derived from EXAFS spectra. J Phys C 12:2465–2473

Cohen SG, Bauminger ER, Nowik I, Ofer S, Yariv J (1981) Dynamics of the iron-containing core in crystals of the iron storage protein, ferritin, through Mössbauer spectroscopy. Phys Rev Lett 46:1244–1248

Cupane A, Leone M, Vitrano E, Cordone L (1995) Low temperature optical absorption spectroscopy: an approach to the study of stereodynamic properties of heme proteins. Eur Biophys J 23:385–398

Dimakis N, Bunker G (1998) Ab initio single- and multiple-scattering EXAFS Debye-Waller factors: Raman and infrared data. Phys Rev B 58:2467–2475

Diop D, Grisenti R (1995) EXAFS Debye-Waller factors of ZnSe. Physica B 208–209:164–166

Di Pace A, Cupane A, Leone M, Vitrano E, Cordone L (1992) Protein dynamics: vibrational coupling, spectral broadening mechanisms, and anharmonicity effects in carbonmonoxy heme proteins studied by the temperature dependence of the Soret band lineshape. Biophys J 63:475–484

Doster W, Cusack S, Petry W (1989) Dynamical transition of myoglobin revealed by inelastic neutron scattering. Nature 357:754–756

Frauenfelder H, Petsko GA, Tsernoglou D (1979) Temperature dependent X-ray diffraction as a probe of protein structural dynamics. Nature 280:558–563

Gurman SJ (1988) The small atom approximation in EXAFS and surface EXAFS. J Phys C 21:3699–3717

Gurman SJ, Binsted N, Ross I (1984) A rapid, exact curved-wave theory for EXAFS calculations. J Phys C 17:143–151

Gurman SJ, Binsted N, Ross I (1986) A rapid, exact curved-wave theory for EXAFS calculations: II. The multiple-scattering contributions. J Phys C 19:1845–1861

Joyner RW, Martin KJ, Meehan P (1987) Some applications of statistical test in analysis of EXAFS and SEXAFS data. J Phys C 20:4005–4012

Kendrew JC, Parrish RG (1956) The crystal structure of myoglobin. III. Sperm-whale myoglobin. Proc R Soc London Ser A 238:305–324

Kidera A, Go N (1992) Normal mode refinement: crystallographic refinement of protein dynamic structure. 1. Theory and test by simulated diffraction data. J Mol Biol 225:457–475

Krupyanskii YuF, Parak FG, Goldanskii VI, Mössbauer RL, Gaubmann EE, Engelmann H, Suzdalev IP (1982) Investigation of large intramolecular movement within metmyolobin by Rayleigh scattering of Mössbauer radiation. Z Naturforsch C 37:57–62

Lee PA, Beni G (1977) New method for the calculation of atomic phase shifts: application to extended x-ray absorption fine structure (EXAFS) in molecules and crystals. Phys Rev B 15:2862–2883

Lee PA, Pendry JB (1975) Theory of extended x-ray absorption fine structure. Phys Rev B 11:2795–2811

Lytle FW, Sayers DE, Stern EA (1989) Report of the international workshop on standards and criteria in X-ray absorption spectroscopy. Physica B 158:701–722

Melchers B, Knapp EW, Parak F, Cordone L, Cupane A, Leone M (1996) Structural fluctuations of myoglobin from normal-modes, Mössbauer, Raman, and absorption spectroscopy. Biophys J 70:2092–2099

Mössbauer RL (1987) Gamma resonance and X-ray investigations of slow motions in macromolecular systems. Hyperfine Interact 33:199–222

Mössbauer RL, Sharp DH (1964) On the theory of resonant scattering of gamma rays by nuclei bound in crystals. Rev Mod Phys 36:410–417

Nazikkol C (1996) PhD Thesis, Westfälische Wilhelms-Universität Münster

Nolting HF, Hermes C (1992) Documentation for the EMBL EXAFS data analysis and evaluation program package, EXPROG, release 1.0. EMBL, Hamburg

Parak F, Formanek H (1971) Untersuchung des Schwingungsanteils und des Kristallgitterfehleranteils des Temperaturfaktors in Myoglobin durch Vergleich von Mössbauerabsorptionsmessungen mit Röntgenstrukturdaten. Acta Crystallogr Sect A 27:573–578

Parak F, Frauenfelder H (1993) Protein dynamics. Physica A 201:332–345

Parak F, Frolov EN, Mössbauer RL, Goldanskii VI (1981) Dynamics of metmyoglobin crystals investigated by nuclear gamma resonance absorption. J Mol Biol 145:825–833

Parak F, Knapp EW, Kucheida D (1982) Protein dynamics. J Mol Biol 161:177–194

Parak F, Hartmann H, Aumann KD, Reuscher H, Rennekamp G, Bartunik H, Steigemann W (1987) Low temperature X-ray investigation of structural distributions in myoglobin. Eur Biophys J 15:237–249

Parak F, Ostermann A, Gassmann A, Scherk C, Chong S-H, Kidera A, Go N (1999) Biomolecules: fluctuations and relax-

ations. In: Frauenfelder H, Hummer G, Garcia R (eds) Biological physics: third symposium. American Institute of Physics, Washington, pp 117–127

Pettifer RF, Hermes C (1985) Absolute energy calibration of X-ray radiation from synchrotron sources. J Appl Crystallogr 18:404–412

Poiarkova AV, Rehr JJ (1999) Multiple-scattering x-ray-absorption fine-structure Debye-Waller factor calculations. Phys Rev B 59:948–957

Scherk C, Schmidt M, Nolting HF, Meier B, Parak F (1996) EXAFS investigation of the active site of iron superoxide dismutase of *Escherichia coli* and *Propionibacterium shermanii*. Eur Biophys J 24:243–250

Sevillano E, Meuth H, Rehr JJ (1979) Extended X-ray absorption fine structure Debye-Waller factors. I. Monoatomic crystals. Phys Rev B 20:4908–4911

Sheldrick GM (1993) SHELXL-93. Universität Göttingen

Stern E (1987) Debye-Waller factor in solid state and biological samples. In: Austin R, Buhks E, Chance B, De Vault D, Dutton PL, Frauenfelder H, Gol'danskii VI (eds) Protein structure. Springer, Berlin Heidelberg New York, pp 3–15

Teo BK (1986) EXAFS: basic principles and data analysis. Springer, Berlin Heidelberg New York

Zhang K, Reddy KS, Bunker G, Chance B (1991) Active site conformation in myoglobin as determined by X-ray absorption spectroscopy. Proteins 10:279–286